

Synthesis, characterization and antibacterial activity of colloidal NiO nanoparticles

Khawlah Salah Khashan¹, Ghassan Mohammad Sulaiman^{2*},
Farah Abdul Kareem Abdul Ameer¹ and Giuliana Napolitano³

¹Laser physics Division, Applied Science Department, University of Technology, Baghdad, Iraq

²Biotechnology Division, Applied Science Department, University of Technology, Baghdad, Iraq

³Department of Biology, University of Naples Federico II, Naples, Italy

Abstract: The Colloidal solutions of nickel oxide (NiO) nanoparticles synthesized via Nd-Yag pulse ablation of nickel immersed in H₂O were studied. The created nanoparticles were characterized by UV-VIS absorption, Fourier transform infrared spectroscopy (FTIR) and transmission electron microscope (TEM). FTIR characterization confirms the formation of nickel oxide nanoparticles. The optical band gap values, determined by UV-VIS absorption measurements, are found to be (4.5eV). TEM shows that nanoparticles size ranged from 2-21 nm. The antimicrobial activity was carried out against *pseudomonas aurogenisa*, *Escherichia coli* (gram negative bacteria), *Staphylococcus aureus* and *Streptococcus pneumonia* (gram positive bacteria). The NiO nanoparticles showed inhibitory activity in both strains of bacteria with best selectivity against gram-positive bacteria. The findings of present study indicate that NiO nanoparticles could potentiate the permeability of bacterial cell wall, and remarkably increase the accumulation of amoxicillin in bacteria, suggesting that NiO nanoparticles together with amoxicillin would facilitate the synergistic impact on growth inhibition of bacterial strains.

Keywords: NiO nanoparticles; pulsed laser ablation in liquid (PLAL); antibacterial activity.

INTRODUCTION

Nanomaterials such as nanoparticles (NPs), nanowires and nanotubes have unique physical and chemical properties (Gopal *et al.*, 2009) that are different from those of bulk materials. Because of these facts, wide variety of techniques for the prepared of nanomaterials were developed (Gondal *et al.*, 2012) such as pulsed laser deposition (Donnelly *et al.*, 2007), chemical reduction (She *et al.*, 2010), photo-reduction (Jia *et al.*, 2006), electrochemical reduction (Lim *et al.*, 2006), sol-gel (Mallick and Sahu, 2012), Spray Pyrolysis (Wang *et al.*, 2005) and laser ablation method (Mahfouz *et al.*, 2008). Nickel oxide (NiO) with a wide band gap (3.6-4.0 eV) (Gondal *et al.*, 2012) has received significant attention as a strong nominee for different applications such as solar cells (Mori *et al.*, 2008), catalysis (Harraz *et al.*, 2010), gas sensors (Aslania *et al.*, 2011) and antibacterial applications (Hajjipour *et al.*, 2012).

Pulsed laser ablation in liquid media (PLAL) has become an increasingly important alternative approach for synthesis of colloidal suspensions, usually in a one step top-down procedure with novel functional properties (Gopal *et al.*, 2009; Acacia *et al.*, 2010). The main benefits of this method are simplicity (Gondal *et al.*, 2012), low cost method and not require high vacuum pumping systems hence it is considered as a green method (Semaltianos *et al.*, 2010). In PLAL, the size and shape of

the produced nanoparticles can be controlled by using a variety types of liquid and a range of laser parameters such as wavelength, ablation time, pulse energy, etc. (Haram and Ahmad, 2013). The nanoparticles obtained by this technique are easier to handle (Gopal *et al.*, 2009).

Highly ionic nanoparticles metal oxides may be particularly important antimicrobial agents as they can be prepared with unusual crystal morphologies and extremely high surface areas (Hrenovic *et al.*, 2012). The antibacterial activity of such nanoparticles depends on their stability, size, and concentration added to the bacterial growth medium, since this provides greater retention time for interaction of bacterium nanoparticles (Azam *et al.*, 2012).

This study was focused on the generated NiO colloidal NPs with effect of changing the ablation time and laser energy on the synthesized nanoparticles in liquid medium by studying the optical and structural characterization of NiO NPs prepared by laser ablation in liquid. Also, the antibacterial activities of these NiO colloidal NPs with or without amoxicillin on cultures of Gram-negative and Gram-positive bacteria were investigated.

MATERIALS AND METHODS

Preparation of colloidal NPs

Nickel targets in the form of pellet was placed at the bottom of glass vessel containing 1ml of deionized water of height 2mm from the target surface as shown in experimental setup in fig. 1. The nickel was irradiated

*Corresponding author: e-mail: gmsbiotech@hotmail.com

with pulsed Q-switched Nd: YAG laser (1064nm, pulse duration=9 ns, repetition rate 1Hz and with built in lens of 120 mm in focal length) operating at different energies (80 and 200mJ) for different ablation time (10, 20min). Each target sample was weighed before and after the ablation by a digital weigher to determine the mass concentration.

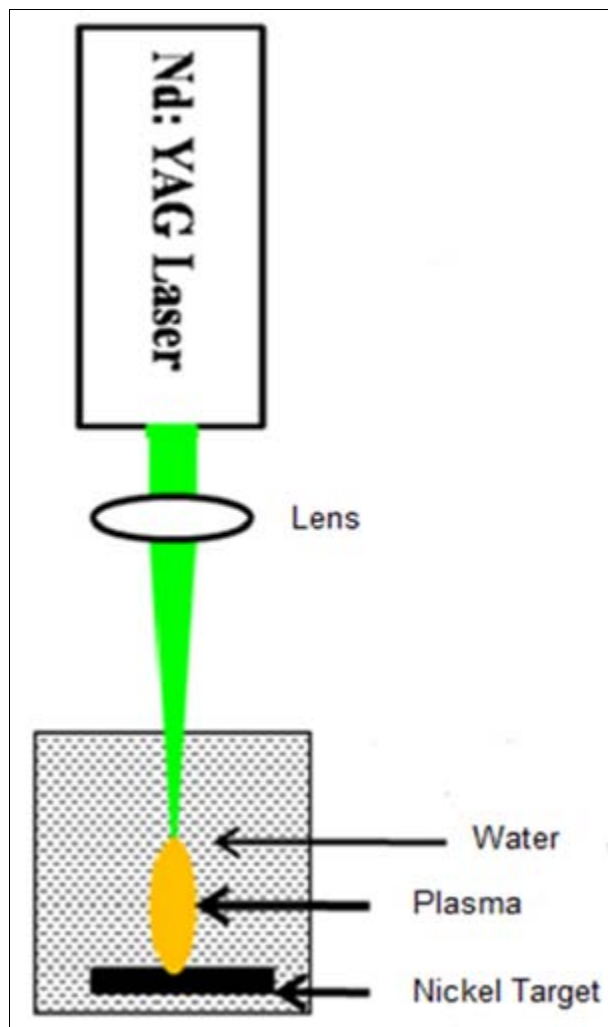


Fig. 1: The schematic of the experimental setup (Nath and Khare, 2011).

Characterization of NPs

The colloid of synthesized nanoparticles was characterized by using optical and structural techniques. For recording the FTIR spectrum, the (Testscan Shimadzu FTIR 8000 series) scans of the FTIR measurements are performed over range between (450-4000) cm⁻¹ for suspension to confirm the formation of nickel oxide nanoparticles. The optical absorption spectrum of NiO nanoparticles was recorded by single beam spectrophotometer (type UIR-210A SHIMADZU) within the wavelength ranges (200-500 nm). The optical band gap was determined graphically by the Tauc plot. TEM analysis was used to determine the particles size and morphology of NPs.

Antimicrobial activity of NPs

The nickel nanoparticles were tested for antimicrobial activity by broth medium methods against *Pseudomonas aeruginosa*, *Escherichia coli* (gram negative bacteria), *Staphylococcus aureus* and *Streptococcus pneumonia* (gram positive bacteria). The bacterial suspension was prepared and adjusted by comparison against 0.5 McFarland turbidity standard (5x 10⁷ cell ml⁻¹) tubes. Both bacterial strains were sub-culture on nutrient broth. The broth was inoculated with 0.2ml of bacterial strains, then 0.5ml of nickel nanoparticles at concentration 400, 600 or 1000µg ml⁻¹ were added. The tubes were incubated for 24h at 37°C. The bacterial growth in broth medium was measured by optical density at 600nm wavelength. The mean values of inhibition were calculated from triple reading in each test. To investigate the inhibition rate of nickel nanoparticles combined with or without amoxicillin, the final concentrations of amoxicillin at 15 or 30µg ml⁻¹ (dissolved in DW) and Ni nanoparticles at 1000µg ml⁻¹ were used. The experiments were repeated in three replicates and, the inhibition efficiency (%) was expressed as follows:

$$\text{Inhibition Efficiency (\%)} = \left(\frac{(A) \text{ Test}}{(A) \text{ Control}} \right) \times 100$$

Where (A) test and (A) control represent the optical density at 600 nm wavelength.

STATISTICAL ANALYSIS

The grouped data were statistically evaluated using ANOVA and one tailed unpaired Student's t-test for significance testing and p≤0.05 is considered significant. Values are presented as the mean ± S.D. of the three replicates of each experiment.

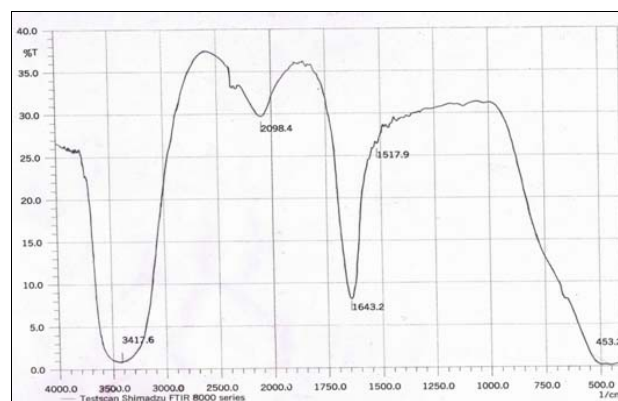


Fig. 2: FTIR spectrum of NiO nanoparticles prepared using laser ablation of nickel target with Nd: YAG of energy 80mJ in deionized water for 10min.

RESULTS

Fig. 2 shows the FTIR spectrum NiO nanoparticles colloidal solution prepared using laser ablation of nickel target with Nd: YAG of energy 80mJ in deionized water for 10 min. The spectrum was recorded in the range (450-4000cm⁻¹).

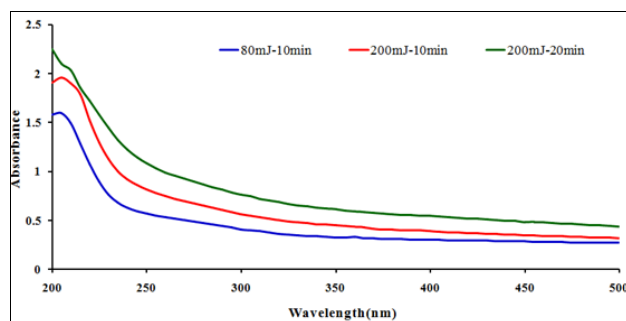


Fig. 3: UV-Vis absorption spectrum of NiO nanoparticles colloids prepared by Nd: YAG laser ablation of nickel in deionized water.

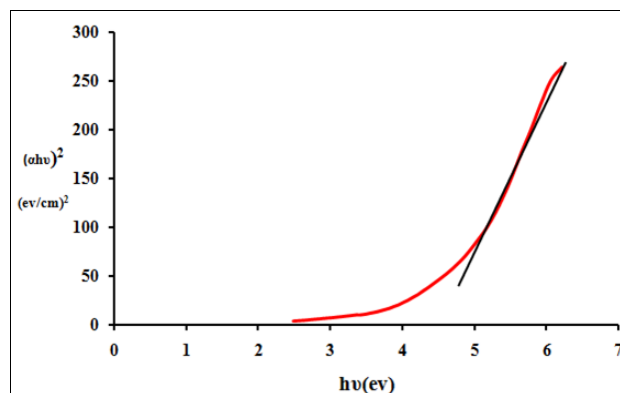


Fig. 4: Tauc plot of UV-Visible absorption data of as colloidal NiO nanoparticles.

The UV-Vis absorption spectra is recorded in the wavelength region of 200-500nm for the colloidal solution prepared in deionized water at two different ablation time by the output of Nd: YAG laser (1064nm) with energy 80mJ and for with energy 200mJ for 10min as shown in fig. 3. The optical band gap of the produced NPs is calculated Tauc's relation

$$(\alpha h\nu)^n = A(h\nu - E_g)$$

Where $h\nu$ is a photon energy, E_g is optical band gap of NPs, A is a constant of effective masses associated with the valance and conduction bands, n is number that determines the type of electronic transition causing the absorption and takes values 2 or $\frac{1}{2}$ depending whether transition is direct or indirect respectively. The best linear line is obtained by plotting $(\alpha h\nu)^2$ against $h\nu$ indicating that the band gap of colloids NPs is direct transition. This is shown in fig. 4. The morphologies of nanoparticles were observed by TEM of samples prepared at 200mJ and for 10 min ablation time were shown in fig. 5.

The optical density of the bacterial cultures in liquid nutrient medium was measured using UV-Vis spectrophotometer, with the measuring wavelength set at 600 nm. Based on the data derived from the liquid nutrient medium experiments, we were able to see that the

bacterial cell number was decreased slightly in all types of bacteria and the inhibition was concentration dependant manner (figs. 6 and 7).

As shown in fig. 7, the $1000\mu\text{g ml}^{-1}$ was the best concentration of nickel nanoparticles for suppressing growth of bacterial strains. It is recorded that concentration of nickel nanoparticles are effective bactericidal agent for both gram positive and gram negative strains but the activity against gram positive bacteria was more than that recorded in other species of gram negative bacteria. On the basis of these findings, the inhibitory effect of amoxicillin on all pathogenic bacteria in the absence and presence of Ni nanoparticles has been further discovered. As shown in fig. 8, the present studies indicate that inhibition efficiency of bacterial growth could be remarkably enhanced in the presence of amoxicillin together with Ni nanoparticles as compared with the activity of either relevant amoxicillin or Ni nanoparticles alone, where the inhibition rate of Ni nanoparticles alone to *S. pneumonia* is 10%, but the relevant inhibition efficiency was increased from 15% ($15\mu\text{g ml}^{-1}$ of amoxicillin) to 35% ($30\mu\text{g ml}^{-1}$ of amoxicillin in the presence of Ni nanoparticles), and from 28% ($30\mu\text{g ml}^{-1}$ of amoxicillin) to 45% ($30\mu\text{g ml}^{-1}$ of amoxicillin in the presence of Ni nanoparticles). Followed by *S. aureus* (fig. 8; D), *E. coli* (fig. 8; B) and then *P. aurogenousa* (fig. 8; A). The t-test results suggest that it has great statistical difference as compared to the amoxicillin or Ni nanoparticles alone ($p \leq 0.05$).

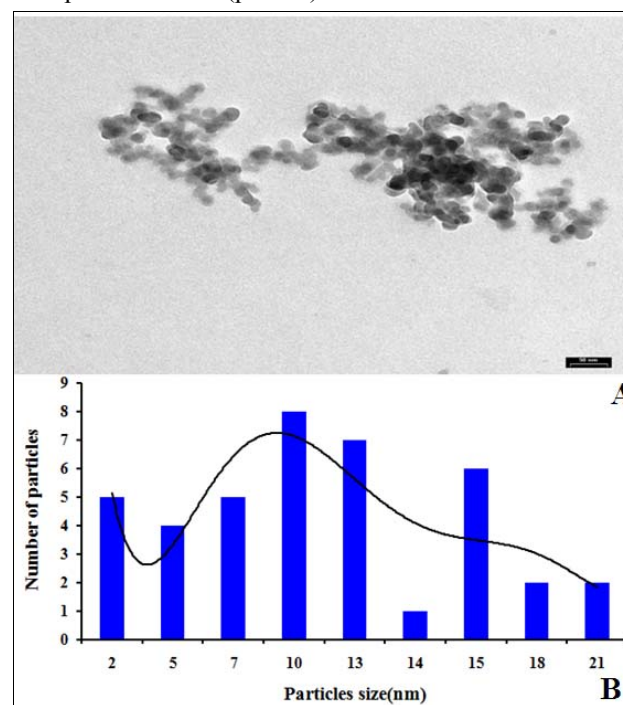


Fig. 5: (a) TEM image of sample, bar 50 nm (b) Particle size distribution of sample.

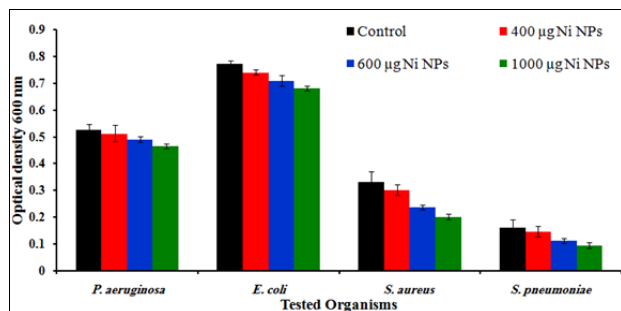


Fig. 6: Antibacterial properties of NiO nanoparticles in Gram negative and positive bacteria. Error bars indicate standard deviation.

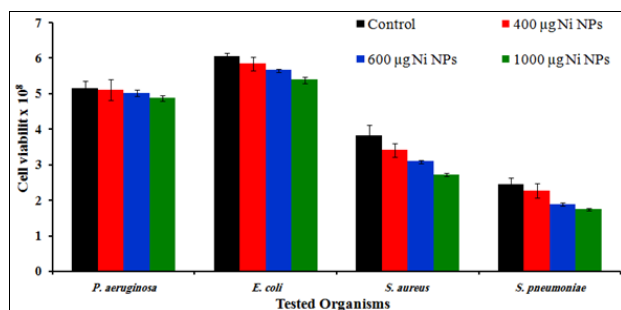


Fig. 7: NiO nanoparticles effect against cell viability of Gram negative and positive bacteria. Error bars indicate standard deviation.

DISCUSSION

The FTIR shows the peaks at 3417cm^{-1} , 1643cm^{-1} , 453cm^{-1} . The intense and wide peak centered at 3417cm^{-1} assigned to O-H stretching, and the peak at 1643cm^{-1} corresponds to the H-O-H bending mode. The band at around 453cm^{-1} is attributed to Ni-O bending vibration. These results agree with other researches (Wang *et al.*, 2005).

The Optical absorption spectra exhibit structure broad stretches have intensity decreases continuously higher than 210nm. Therefore, the information about the size and /or morphology of the metal particles not well documented. Nevertheless, one sees that the UV light absorption enhances with the metal abundance within the liquid. The value of optical band gap of NiO colloids NPs is determined from the extrapolation of the straight line at $\alpha=0$ and which is found to be 4.5eV. The band gap for bulk NiO is 3.74eV (Rifaya *et al.*, 2012), this yields a shift for NiO nanoparticles. The morphologies of nanoparticles were observed by TEM of samples prepared at 200mJ and for 10 min ablation time. From fig. 5a, the products are pseudo-round-shaped (Mahfouz *et al.*, 2008). There are little aggregations observed in the prepared sample. The distribution of particle size is measured from fig. 5a. fig. 5b shows the particle size distribution histogram for NiO nanoparticles. It is a narrow size distribution and the diameter of nanoparticles ranged between 2 and 21 nm

with average size at 12 nm. These results are agreed with previous work of (Liu *et al.*, 2008).

The antibacterial activity against different pathogenic bacteria showed that amoxicillin together with NiO nanoparticles could inhibit the bacterial growth more efficiently than that observed in the single addition of amoxicillin and NiO nanoparticles, which indicates that NiO nanoparticles and amoxicillin have synergic activity on suppressing the bacterial growth. It was also observed that synergic effects are very effective bactericidal agent for both gram negative and gram-positive strains, which demonstrated that NiO nanoparticles can efficiently enhance the penetration and uptake of amoxicillin into bacterial cell membrane. Also, NiO nanoparticles have large surface area available to facilitate the interactions that increases bactericidal effect compared to large sized particles; hence they impart increment in cytotoxicity to the microorganisms (Baker *et al.*, 2005).

The mechanism by which the nanoparticles penetrates into bacteria is not well known, but studies suggest that when bacterial culture were treated with nanoparticles, changes takes place in its membrane morphology and cause a significant increase in its permeability affecting proper transport through the plasma membrane, leaving the bacterial cells incapable of properly regulating transport through the plasma membrane, resulting into cell death (Stoimenov *et al.*, 2002). It is suggested that nickel nanoparticles due to its small size penetrated the bacterial cell membrane and binds to functional groups of proteins, resulting in protein denaturation (Spadaro *et al.*, 1974) and might caused damage to the bacterial cell by interacting with phosphorous and sulphur containing compounds such as DNA causing bacterial cell death (Kokkoris *et al.*, 2002; Morones *et al.*, 2005).

CONCLUSION

The present work shows that nickel oxide nanoparticles can be easily produced by laser ablation of nickel metal in water. Variation of size and shape of nanoparticles has been found to depend on the duration of ablation and laser energy. FTIR spectra confirm the bond between nickel and oxygen at around $(418-453)\text{cm}^{-1}$. UV-Vis absorption spectrum indicates the optical band gap, which is about 4.5 eV. Antibacterial activity experiments performed on various microorganisms clearly demonstrated the efficiency of NiO nanoparticles against bacterial growth due to high concentration and smaller particle size of the nanoparticles. The results suggest that NiO nanoparticles together with amoxicillin have synergic activity on cell membrane of bacteria, and Ni nanoparticles can efficiently enhance the penetration and uptake of amoxicillin into bacteria cell, making it a promising platform for biomedical applications.

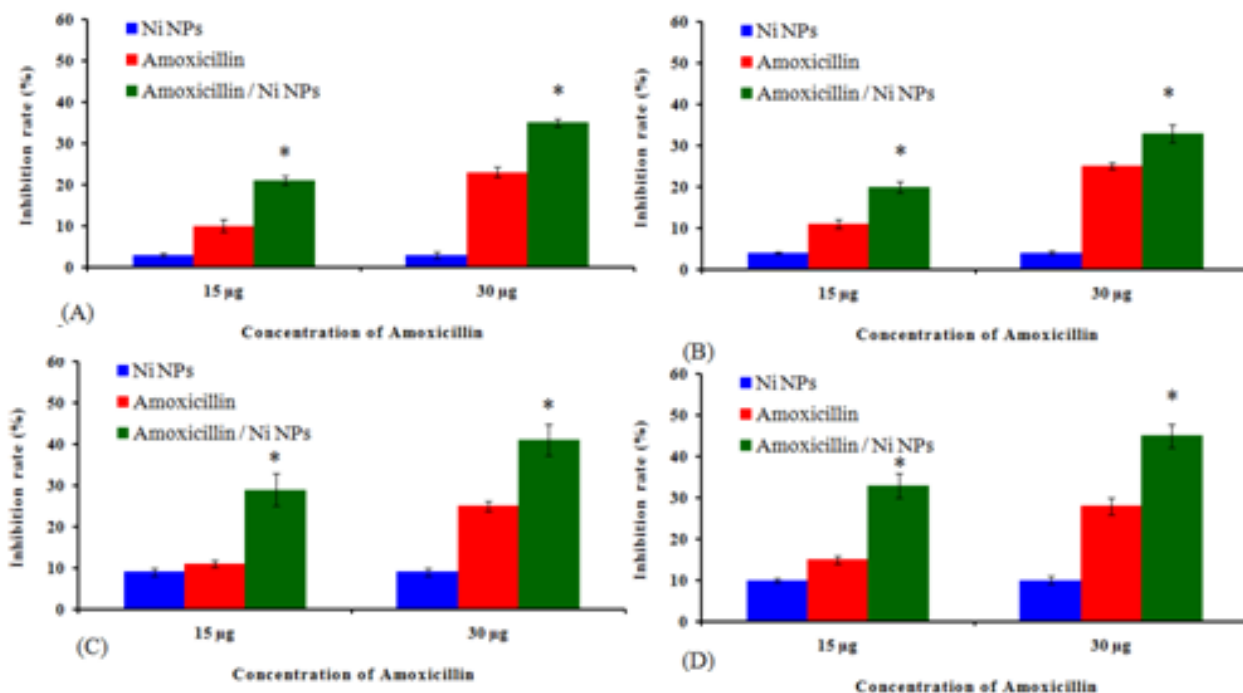


Fig. 8: The inhibition rate of tested bacteria after treatment with amoxicillin together with Ni nanoparticles, where * represents $p \leq 0.05$. (A) *P. aurogenosa*, (B) *E. coli*, (C) *S. aureus* and (D) *S. pneumoniae*. Error bars indicate standard deviation.

ACKNOWLEDGEMENTS

This work was supported by Department of Applied Science, University of Technology, Iraq, Baghdad, Project No. AS/2156/2012.

REFERENCES

- Acacia N, Barreca F, Barletta E, Spadaro D, Currò G and Neri F (2010). Laser ablation synthesis of indium oxide nanoparticles in water. *Appl. Surf. Sci.*, **256**: 6918-6922.
- Aslania A, Oroojpour V and Fallahi M (2011). Sonochemical synthesis, size controlling and gas sensing properties of NiO nanoparticles. *Appl. Surf. Sci.*, **257**: 4056-4061.
- Azam A, Ahmed AS, Oves M, Khan MS and Memic A (2012). Size-dependent antimicrobial properties of CuO nanoparticles against Gram-positive and -negative bacterial strains. *Int. J. Nanomed.*, **7**: 3527-3535.
- Baker C, Pradhan A, Pakstis L, Pochan D J and Shah S I (2005). Synthesis and antibacterial properties of silver nanoparticles. *J. Nanosci. Nanotechnol.*, **5**: 244-249.
- Donnelly T, Krishnamurthy S, Carney K, Evoy N Mc and Lunney JG (2007). Pulsed laser deposition of nanoparticle films of Au. *Appl. Surf. Sci.*, **254**: 303-306.
- Gondal MA, Saleh TA and Drmish QA (2012). Synthesis of nickel oxide nanoparticles using pulsed laser ablation in liquids and their optical characterization. *Appl. Surf. Sci.*, **258**: 6982-6986.
- Gopal R, Singh MK, Agarwal A, Singh SC and Swarnkar RK (2009). Synthesis of nickel nanomaterial by pulsed laser ablation in liquid medium and its characterization. *AIP. Conf. Proc.*, **1147**: 199-204.
- Hajipour MJ, Fromm KM, Ashkarran AA, de Aberasturi DJ, de Larramendi IR, Rojo T, Serpooshan V, Parak WJ and Mahmoudi M (2012). Antibacterial properties of nanoparticles. *Trends Biotechnol.*, **30**: 499-511.
- Haram N and Ahmad N (2013). Effect of laser fluence on the size of copper oxide nanoparticles produced by the ablation of Cu target in double distilled water. *Appl. Phys. A.*, **111**: 1131-1137.
- Harraz FA, Mohamed RM, Shawky A and Ibrahim IA (2010). Composition and phase control of Ni/NiO nanoparticles for photocatalytic degradation of EDTA. *J. Alloys Comp.*, **508**: 133-140.
- Hrenovic J, Milenkovic J, Daneu N, Kepcija RM and Rajic N (2012). Antimicrobial activity of metal oxide nanoparticles supported onto natural clinoptilolite. *Chemosphere*, **88**: 1103-1107.
- Jia H, Zeng J, Song W, An J and Zhao B (2006). Preparation of silver nanoparticles by photo-reduction for surface-enhanced Raman scattering. *Thin. Solid Films*, **496**: 281-287.
- Kokkoris M, Trapalini CC, Kossionides S, Vlastou R, Nsouli B, Grotzschel R, Spartalis S, Kordas G and Paradellis Th (2002). RBC and HIRBS studies of

- nanostructured AgSiO₂ Sol-Gel thin coatings. *Nucl. Instr. Meth. Phys. Res. B.*, **188**: 67-72.
- Lim PY, Liu RS, She PL, Hung CF and Shih HC (2006). Synthesis of Ag nanospheres particles in ethylene glycol by electrochemical-assisted polyol process. *Chem. Phys. Lett.*, **420**: 304-308.
- Liu B, Hu Z, Che Y, Chen Y and Pan X (2007). Nanoparticle generation in ultra fast pulsed laser ablation of nickel. *Appl. phys. lett.*, **90**: 044103.
- Mahfouz R, Cadete Santos Aires FJ, Brenier A, Jacquier B and Bertolini JC (2008). Synthesis and physico-chemical characteristics of nanosized particles produced by laser ablation of a nickel target in water. *Appl. Surf. Sci.*, **254**: 5181-5190.
- Mallick P and Sahu S (2012). Structure, microstructure and optical absorption analysis of CuO nanoparticles synthesized by Sol-Gel route. *Nanosci. Nanotechnol.*, **2**: 71-74.
- Mori S, Fukuda S, Sumikura S, Takeda Y, Tamaki Y, Suzuki E and Abe T (2008). Charge-transfer processes in dye-sensitized NiO solar cells. *J. Phys. Chem. C.*, **112**: 16134-16139.
- Morones JR, Elechigierra JL, Caacho A, Holt K, Kouri J B, Ramirez JT and Yacaman MJ (2005). The bactericidal effect of silver nanoparticles. *J. Nanotechnol.*, **16**: 2346-2353.
- Nath A and Khare A (2011). Size induced structural modifications in copper oxide nanoparticles synthesized via laser ablation in liquids. *J. Appl. Phys.*, **110**: 043111.
- Rifaya MN, Theivasanthi T and Alagar M (2012). Chemical capping synthesis of nickel oxide nanoparticles and their characterizations studies. *Nanosci. Nanotechnol.*, **2**: 134-138.
- Semaltianos N G, Logothetidis S, Frangis N, Tsiaoussis I, Perrie W, Dearden G and Watkins KG (2010). Laser ablation in water: A route to synthesize nanoparticles of titanium monoxide. *Chem. Phys. Lett.*, **496**: 113-116.
- She Y Y, Yang J and Qiu K Q (2010). Synthesis of ZnS nanoparticles by solid-liquid chemical reaction with ZnO and Na₂S under ultrasonic. *Trans. Nonferrous Met. Soc.*, **20**: S211-S215.
- Spadaro JA, Berger TJ, Barranco SD, Chapin SE and Becker RO (1974). Antibacterial effects of silver electrodes with weak direct current. *J. ACS Soc. Microbiol.*, **6**: 637-642.
- Stoimenov PK, Klinger RL, Marchin GL and Klabunde K (2002). Metal oxide nanoparticles as bactericidal agents. *Langmuir*, **18**: 6679-6686.
- Wang WN, Lenggoro IW, Terashi Y, Kim TO and Okuyama K (2005). One-step synthesis of titanium oxide nanoparticles by spray pyrolysis of organic precursors. *Mat. Sci. Eng. B.*, **123**: 194-202.
- Wang Y, Zhu J, Yang X, Lu L and Wang X (2005). Preparation of NiO nanoparticles and their catalytic activity in the thermal decomposition of ammonium perchlorate. *Thermochimica. Acta.*, **437**: 106-109.